



Dual-Band Bandpass Filter Based on Coupled Complementary Hairpin Resonators (C-CHR)

F. Khamin-Hamedani* and Gh. Karimi***(C.A.)

Abstract: A novel dual-band bandpass filter (DB-BPF) with controllable parameters in design process and a compact structure is introduced in this paper. The total structure includes open-circuited and short circuited coupled-lines, leading to a compact circuit. The resonance frequencies, insertion loss and quality factor can be independently controlled by adjusting the coupled lines. In order to eliminate the magnetic and electric coupling effects, the virtual grounds are placed in coupled complementary hairpin resonator. To verify the validity of the design approach, a DB-BPF centring, at 3.5 and 5 GHz with respective insertion losses of 0.7 and 0.58dB for WiMAX (IEEE 802.16 band) and WLAN (IEEE 802.11 band) applications has been designed and fabricated, whose the measured results confirm the electromagnetic simulation.

Keywords: Micro-Strip Bandpass Filter, Coupled Complementary Hairpin Resonator (C-CHR), Admittance Analysis, Two-Band, WLAN Systems, WiMAX Systems.

1 Introduction

HIGH performance multi-bandpass filters (MBPFs) are highly desirable for the next stage of modern wireless communication systems in the radio frequency band that can operate at multiple frequencies. The most common method to design a multi-band filter is based on stub loaded resonator (SLR) [1-3], or stepped impedance resonator (SIR) [4-6]. Another method to implement multi-band filter is to combine several resonators to achieve a multi-band band-pass filter [7, 8]. In [9], a multi-band BPF is accomplished by combining band-pass and band-stop filters. However, the final structure is large because of the number of resonators used. Also, degrees of freedom in designing each passband are insufficient. Slow-wave resonators are not applicable for high fractional bandwidths although providing excellent wideband response.

Multilayer structures prepare many drawbacks such as complex configuration and fabrication difficulties while realizing that lumped element may not always be practical. The parallel-coupled micro-strip BPF, due to its planar structure and easy design procedures, has been one of the most commonly used filters for the RF systems [10, 11].

A dual-band BPF with independently controllable passbands in design process is presented in this work, using based on coupled complementary hairpin resonators (C-CHR). With the assistance of hairpin lines, good performances at passband come up. The final structure of the filter has performances like compact size ($13.6 \times 19.6 \text{ mm}^2$), and appropriate insertion loss ($< 0.7 \text{ dB}$).

2 Filter Analysis and Design

Fig. 1 shows a layout of the proposed dual-band C-CHR micro-strip filter using short-circuited and open-circuited coupled-lines. Short-circuited and open-circuited coupled-lines are used to realize the strong capacitive effects and therefore electric coupling and finally the high quality factor.

The basic structure of the proposed bandpass filter (BPF) can be shown as Fig. 2(a). This simplified structure is composed of coupled hairpin resonators, where Z_e , Z_o are the even and odd modes characteristic

Iranian Journal of Electrical and Electronic Engineering, 2018.

Paper first received 05 April 2018 and accepted 24 May 2018.

* The author is with the Department of Electronic, College of Engineering, Kermanshah Branch, Islamic Azad University, Kermanshah, Iran.

E-mail: farnazkhamin@iauksh.ac.ir.

** The author is with the Department of Electrical, Faculty of Engineering, Razi University, Kermanshah, Iran.

E-mail: ghkarimi@razi.ac.ir.

Corresponding Author: Gh. Karimi.

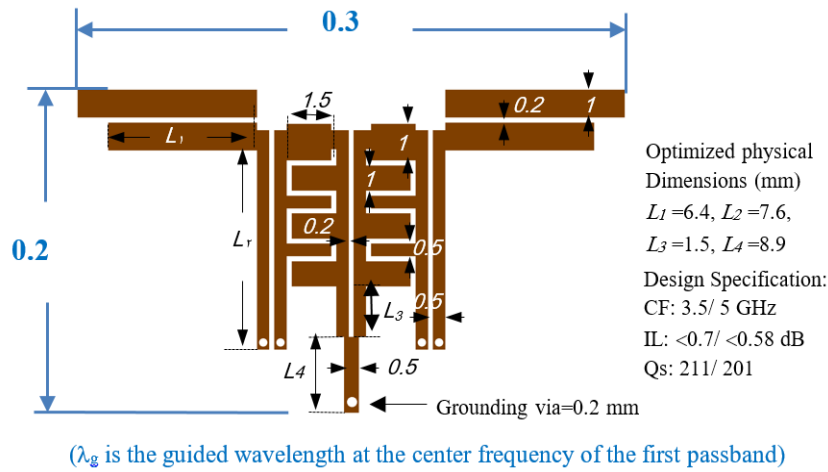


Fig. 1 The proposed Dual-band C-CHR filter.

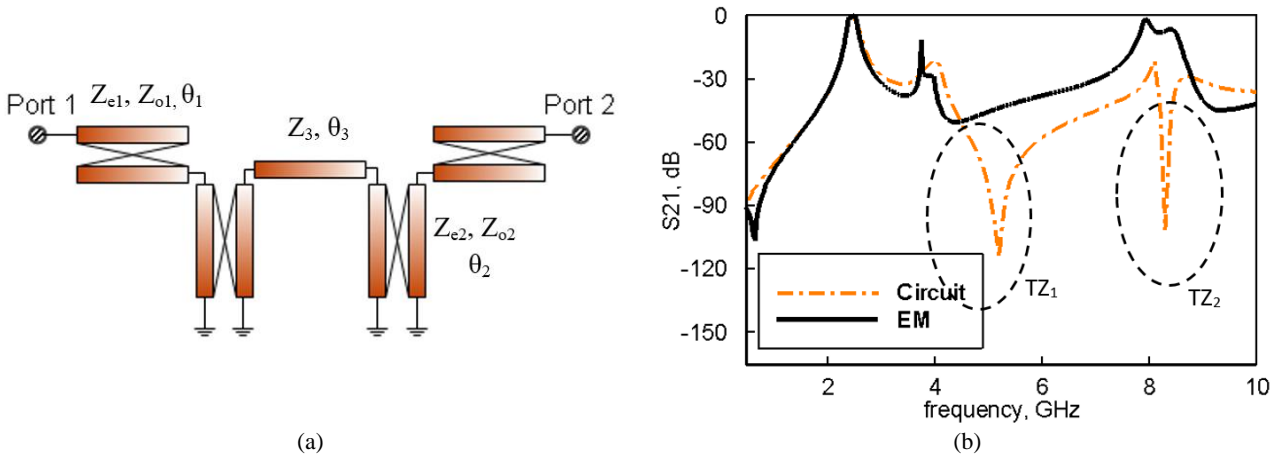


Fig. 2 a) Basic structure and b) Simulated results using ideal transmission-line models of proposed BPF.

impedance and θ is the electric length of the coupled line sections. In the basic design, the use of short circuited lined has led to the creation of two transmission zeros (TZs), which can improve the stopband as shown in Fig. 2(b). Short circuits in the circuit model in Fig. 2(a) are replaced with grounding via holes in EM simulations.

In order to create another passband, multiple coupled lines are added to the basic proposed BPF, as shown in Fig. 3(a). Coupled hairpin resonators are introduced to form the 1st passband, while short-circuited coupled lines are used to implement the 2nd passband. Also, the simulation S-parameters results in Fig. 3(b) show that the designed dual band bandpass filter (DB-BPF) has a proper stopband.

2.1 Analysis of Peak Frequencies of DB-BPF

Simplified coupling scheme of the final structure of DB-BPF is shown in Fig. 4. If imaginary part of input admittance is equal to zero the main frequency of system can be achieved. As seen in Fig. 4, it is more appropriate to calculate the input impedance. Z_{in} can be

found as the input impedance of port 1, when port 2 is open-circuited.

Z_A can be obtained using the equation shown in Fig. 4, and since port 2 is open circuited, $Y_L = 0$ is considered as:

$$Z_A = -j \left(\frac{Z_{1e} + Z_{1o}}{2} \right) \cot(\theta_1) \quad (1)$$

where Z_e, Z_o are the even and odd modes characteristic impedance and θ is the electric length of the coupled line section.

Also Z_B is calculated by the same equation:

$$Z_B = \frac{Z_A A_2 \sin(2\theta_2) + j [B_2^2 - A_2^2 \cos^2(\theta_2)]}{A_2 \sin(2\theta_2) + j 4Z_A \sin^2(\theta_2)} \quad (2)$$

($A_2 = Z_{2e} + Z_{2o}$), ($B_2 = Z_{2e} - Z_{2o}$)

In the next step:

$$Y_E = Y_{E1} + Y_{E2} = -jY_4 \cot(\theta_4) + Y_3 \frac{Y_B + jY_3 \tan(\theta_3)}{Y_3 + jY_B \tan(\theta_3)}$$

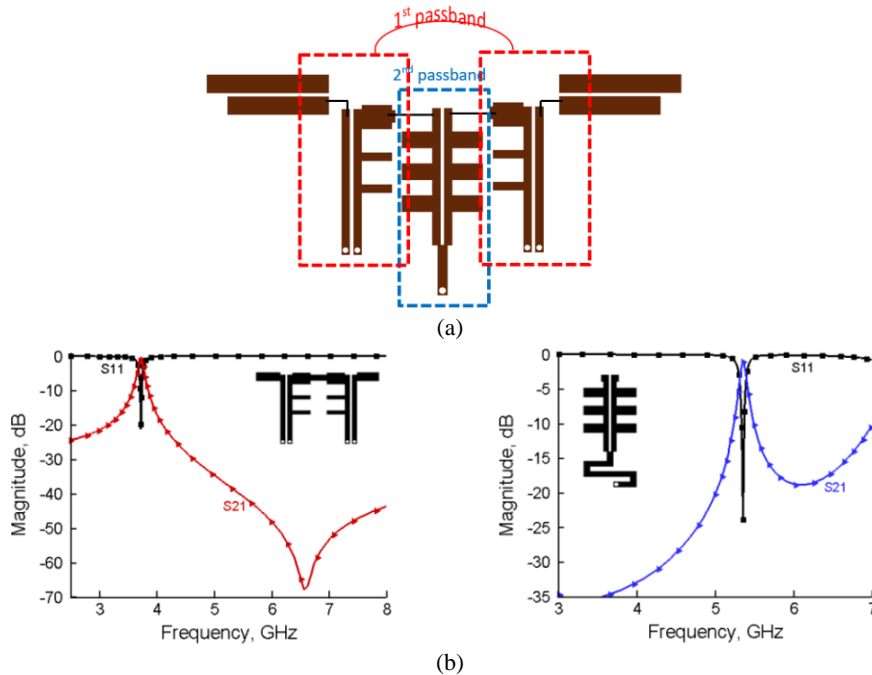


Fig. 3 a) Coupling scheme of the proposed DB-BPF and b) simulated S-parameters of open-circuited and short-circuited coupled lines.

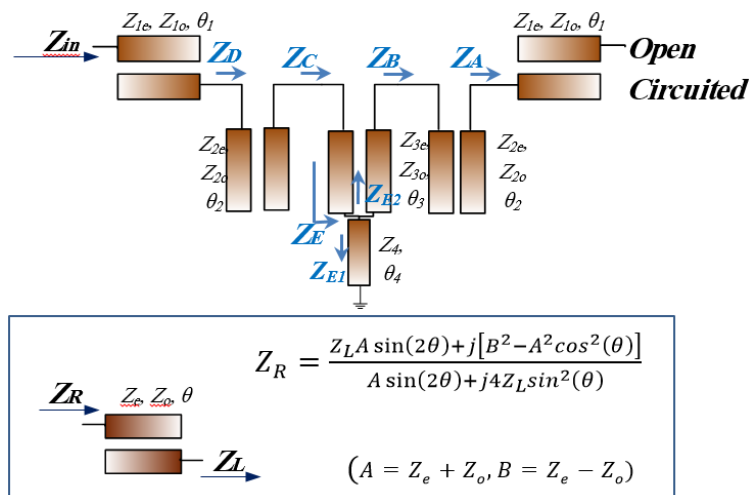


Fig. 4 Simplified coupling schematic of the proposed DB-BPF.

$$\left(Z_E = \frac{1}{Y_E} \right) \quad (3)$$

According to the process of Eqs. (1) and (2) Z_C, Z_D and finally Z_{in} can be obtained:

$$Z_C = Z_3 \frac{Z_E + jZ_3 \tan(\theta_3)}{Z_3 + jZ_E \tan(\theta_3)} \quad (4)$$

$$Z_D = \frac{Z_C A_2 \sin(2\theta_2) + j[B_2^2 - A_2^2 \cos^2(\theta_2)]}{A_2 \sin(2\theta_2) + j4Z_C \sin^2(\theta_2)} \quad (5)$$

Y_{in}, according to the Eqs. (1)-(5) is achieved as mentioned below:

$$Z_{in} = \frac{Z_D A_1 \sin(2\theta_1) + j[B_1^2 - A_1^2 \cos^2(\theta_1)]}{A_1 \sin(2\theta_1) + j4Z_D \sin^2(\theta_1)} \quad (6)$$

(A₁ = Z_{1e} + Z_{1o}), (B₁ = Z_{1e} - Z_{1o})

$$Y_{in} = \frac{1}{Z_{in}} \quad (7)$$

Fig. 5 shows the imaginary part of Y_{in}, which can help to find the main frequencies of BPF, so that these frequencies cause that the admittance, is equal to zero. Also we can see in these figures, the main frequencies can be tuned by altering the electrical length of lines θ₁ and θ₄.

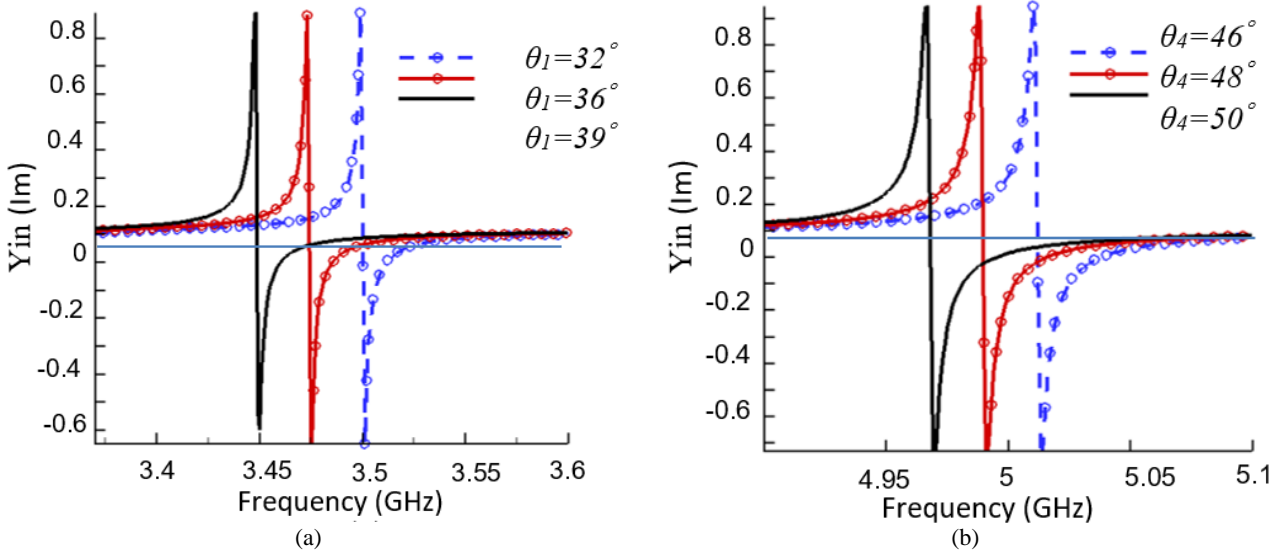


Fig. 5 Input admittance chart under different a) θ_1 and b) θ_4 (θ_1 and θ_4 are the electric lengths as shown in Fig.4).

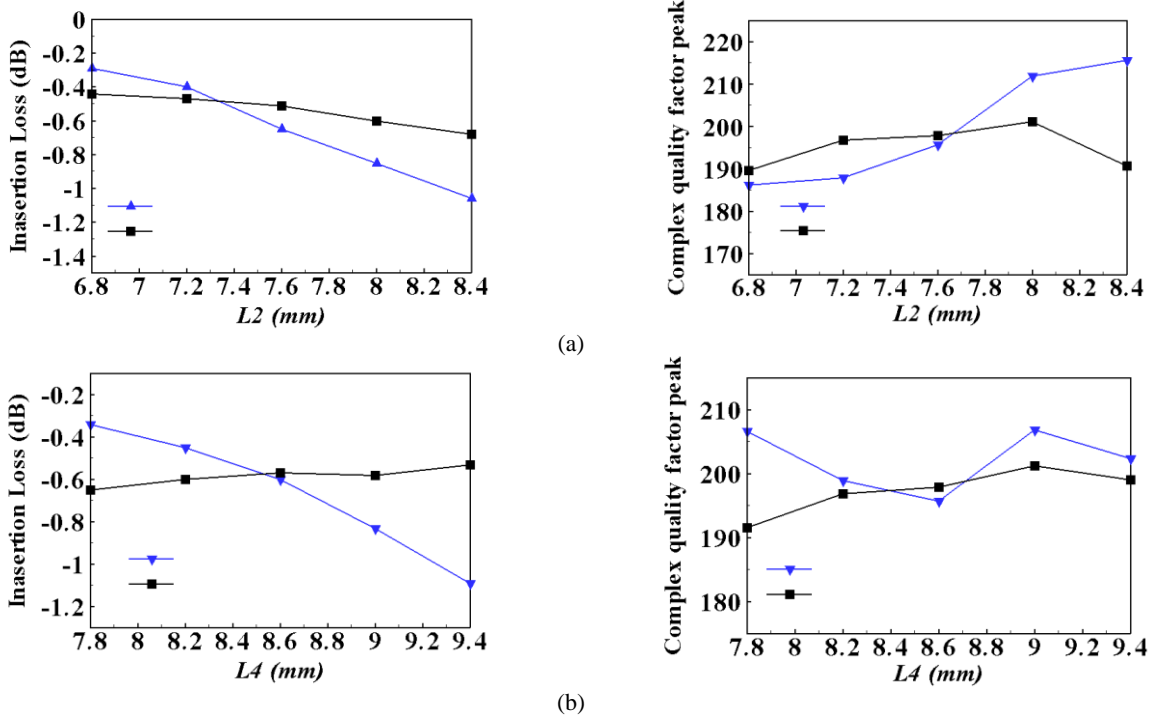


Fig. 6 Variation of insertion loss and complex quality factor against different values of a) L_2 and b) L_4 (L_2 and L_4 are the dimensions of lines as shown in Fig. 1).

2.2 Optimization of Spectrum-Based Quality Factor Q_s and Insertion Loss of DB-BPF

By considering the impedance matrix of the BPF, the spectrum-based quality factor Q_s is defined as [3]

$$Q_s = \frac{\omega_0}{2} \left| \frac{Z'_{11} - Z'_{12}}{Z'_{11} + Z'_{12}} \right| = \frac{\omega_0}{2} \left| \frac{d}{d\omega} \left(\ln \frac{Z_{11}}{Z_{12}} \right) \right| \quad (8)$$

Also, by converting Q_s into a polar form, it can be represented as follows [3]

$$Q_s = \frac{\omega_0}{2} \left| \frac{d}{d\omega} \ln \left| \frac{Z_{11}}{Z_{12}} \right| + j \frac{d}{d\omega} (\angle(Z_{11}) - \angle(Z_{12})) \right| \quad (9)$$

where ω_0 is the center frequency. Eq. (9), clearly indicates that the Q_s relates both of the phase and amplitude effects of the filter. Fig. 6(a) and 6b show that the Q_s -peak value and S_{21} (insertion loss) of the final structure (as shown in Fig. 1) in the two passbands depend on the L_2 and L_4 dimensions.

Fig. 7 shows the simulated Q_s of the DB-BPF, where two Q_s peaks can be observed at 3.5 and 5 GHz, while

Downloaded from ijeee.iust.ac.ir at 22:17 IRST on Thursday January 17th 2019 [DOI: 10.22068/IJEEE.14.4.324]

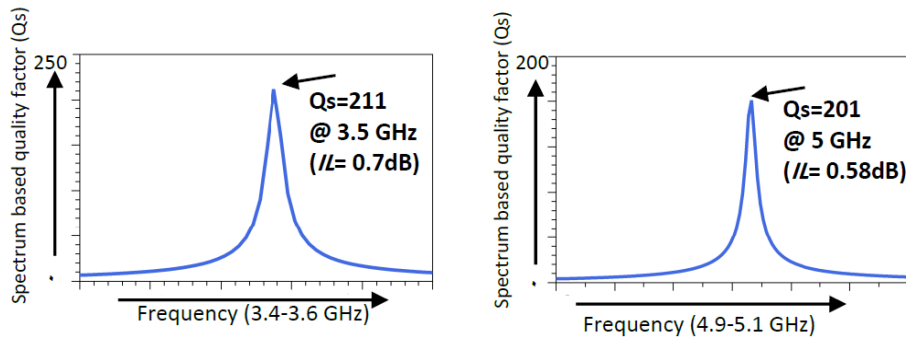


Fig. 7 Spectrum based quality factor (Q_s) of dual-band BPF (IL : Insertion loss).

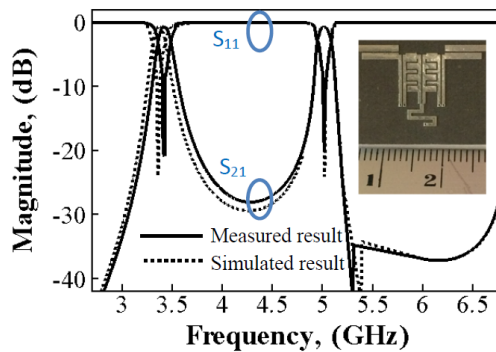


Fig. 8 Photograph, simulated and measured S-parameters of fabricated DB-BPF.

Table 1 Comparison of several multi-band bandpass filters.

Ref.	Centre Frequencies (GHz)	Insertion Loss (dB)	Circuit Size ($\lambda_g \times \lambda_g$)	Independently Controllable Parameters in the Design Process		
				CFs	QFs	ILs
[4]	082/1.67/2.17	0.46/1.05/1.4	0.126×0.108	Y	N	N
[5]	1.8/5.8	1.21/3.89	0.25×0.49	N	Y	N
[6]	2.4/5.8	0.95/1.61	0.68×0.158	N	Y	N
[12]	2.4/3.5/5.5	1.26/1.37/1.41	-	N	N	Y
[13]	2.35/5.2	1.4/1.76	0.21×0.35	N	Y	N
[14]	2.55/3.65	1.22/2.13	0.29×0.41	N	N	N
This Work	3.5/5	0.7/0.58	0.21×0.31	Y	Y	Y

* CFs: Center frequencies, QFs: Quality factors, ILs: Insertion losses, Y: Yes and N: No.

two frequencies have appropriate insertion loss.

3 Simulation and Measurement Results

These theoretical values are used to obtain the final dimensions of the DB-BPF, which is simulated and fabricated using a RT/Duorid 5880 substrate with a relative dielectric constant 2.2 and thickness of 31mil. Fig. 8 presents the photograph of the fabricated filter and simulated/measured S-parameters of the designed DB-BPF. The frequencies of this dual-band bandpass filter are set as 3.5 and 5 GHz that the measured insertion losses for two bands are 0.7/0.58 dB, while the measured return loss is smaller than -20 dB within the pass-bands. The practical size is 13.6×19.6 mm², about 0.21 λ_g ×0.31 λ_g , where λ_g is the guided wavelength at centre frequency of the first passband.

The performance and controllable parameters in the design process of the proposed filter is compared to the other state-of-the-art designs in Table 1. Compared with

the works in [5-6] and [13-14], CFs and ILs of two passbands can be more easily controlled and smaller size is obtained. In [4] compact size is designed, but QFs and ILs are not controllable. Also in [12], ILs of passbands can be optimized, but there isn't any control over the CFs. It can be seen that the proposed filter outperform the others in terms of the insertion loss, size and tuneable to all the three passbands frequencies in design process.

4 Conclusion

This paper presents a compact two-band filter centering at 3.5/5 GHz base on coupled complementary hairpin resonators (C-CHR) suitable for design of multi-order filters. The filter can achieve controllability of the parameters of center frequencies, quality factors and insertion losses in the design process. The selectivity of 1st and 2nd bands is improved by extending the lines of L_1 and L_4 . The filter is fabricated and measured for

WIMAX and WLAN applications. Fabricated filter has simple structure, compact size and low insertion loss so that these performances are very attractive in the practical applications in modern communication systems.

References

- [1] S. Yang, L. Lin, J. Chen, K. Deng and C. H. Liang, "Design of compact dual-band bandpass filter using dual-mode stepped-impedance stub resonators," *Electronics Letters*, Vol. 50, No. 8, pp. 611–613, Apr. 2014.
- [2] X. Y. Zhang, J. X. Chen, Q. Xue and S. M. Li, "Dual-band bandpass filters using stub-loaded resonators," *IEEE Microwave and Wireless Components Letters*, Vol. 17, No. 8, pp. 583–585, Aug. 2007.
- [3] M. Zhou, X. Tang and F. Xiao, "Compact dual-band bandpass filters using novel e-type resonators with controllable bandwidths," *IEEE Microwave and Wireless Components Letters*, Vol. 18, No.12, pp. 779–781, Dec. 2008.
- [4] B. Yu, B. Jia and Z. Zhu, "Compact tri-band bandpass filter with stub loaded stepped impedance resonator," *Electronics Letters*, Vol. 51, No. 9, pp. 7011–7033, Apr. 2015.
- [5] S. B. Zhang and Zhu, "Fully canonical dual-band bandpass filter with $\lambda/4$ stepped impedance resonators," *Electronics Letters*, Vol. 50, No. 3, pp. 192–194, Feb. 2014.
- [6] S. B. Zhang and L. Zhu, "Synthesis design of dual-band bandpass filters with $\lambda/4$ stepped impedance resonators," *IEEE Transactions on Microwave Theory and Techniques*, Vol. 61, No. 12, pp. 1812–1819, May. 2013.
- [7] S. C. Lin, "Microstrip dual/quad-band filters with coupled lines and quasi-lumped impedance inverters based on parallel-path transmission," *IEEE Transactions on Microwave Theory and Techniques*, Vol. 59, No. 8, pp. 1937–1946, 2011.
- [8] S. Zhang and L. Zhu, "Compact tri-band bandpass filter based on resonators with u-folded coupled-line," *IEEE Microwave and Wireless Components Letters*, Vol. 23, No. 5, pp. 258–261, 2013.
- [9] Y. Heng, X. Guo, B. Cao, B. Wei, X. Zhang, G. Zhang and X. Song, "Compact superconducting dual-band bandpass filter by combining bandpass and band-stop filters," *Electronics Letters*, Vol. 49, No. 19, pp. 1230–1232, 2013.
- [10] W. Feng, L. Gu, W. Che and H. Chen, "Tri-band microstrip bandpass filter using input/output cross coupling," *Journal of Electromagnetic Waves and Applications*, pp. 405–409, 2013.
- [11] A. Neghar, O. Aghzot, A. V. Alejos, M. G. Sanches and M. Essaaidi, "Design of compact multiband bandpass filter with suppression of second harmonic spurious by coupling gap reduction," *Journal of Electromagnetic Waves and Applications*, Vol. 29, No. 14, pp. 1813–1828, 2015.
- [12] R. Chatak, M. Pal, P. Sarkar, A. Kumar Aditya and D. R. P. Poddar, "Tri-band bandpass filters using modified tri-section stepped impedance resonator with improved selectivity and wide upper stopband," *IET Microwaves, Antennas & Propagation*, Vol. 7, No. 15, pp. 1187–1193, 2013.
- [13] J. M. Yan, L. Z. Cao, J. Xu, and R. S. Chen, "Design of a fourth-order dual-band bandpass filter with independently controlled external and inter resonator coupling," *IEEE Microwave and Wireless Components Letters*, Vol. 25, No. 10, pp. 642–644, 2015.
- [14] W. Ieu, D. Zhang, D. Zhang and D. Zhou, "Dual-mode dual-band microstrip bandpass filter with multi transmission zeros," *Electronics Letters*, Vol. 53, No. 7, pp. 482–484, 2017.



F. Khamin-Hamedani was born in Kermanshah, Iran in 1980. She received her B.Sc. degree in Electronic Engineering in 2003 from Razi University, Kermanshah, Iran and M.Sc. degree in Electronic Engineering in 2013 from Islamic Azad University, Science and Research Branch, Kermanshah, Iran. She is now a Ph.D. collegian in Electronic Engineering in Department of Electronic, College of Engineering, Kermanshah Branch, Islamic Azad University, Kermanshah, Iran. Her current research interests are RF/Microwave circuit design.



Gh. Karimi was born in Kermanshah, Iran in 1977. He received the B.Sc. and M.Sc. and Ph.D. degrees in Electrical Engineering from Iran University of Science and Technology (IUST) in 1999, 2001 and 2006 respectively. He is currently an Associate Professor in Electrical Department at Razi University, Kermanshah. His research interests include low power Analog and Digital IC design, RF IC design, modeling and simulation of RF mixed signal IC and microwave devices.



© 2018 by the authors. Licensee IUST, Tehran, Iran. This article is an open access article distributed under the terms and conditions of the Creative Commons Attribution-NonCommercial 4.0 International (CC BY-NC 4.0) license (<https://creativecommons.org/licenses/by-nc/4.0/>).